DOI: 10.1002/ejic.201100339

A Porphyrin-Bridged Pd Dimer Complex Stabilizes Gold Nanoparticles

Ilaria Fratoddi,*[a] Chiara Battocchio,[b] Giovanni Polzonetti,[b] Fabio Sciubba,[c] Maurizio Delfini,[a] and Maria Vittoria Russo[a]

Keywords: Gold / Nanoparticles / Porphyrinoids / Palladium / NMR spectroscopy

A porphyrin-bridged bimetallic palladium(II) diphenylacetylide complex and the oligomer with 3–5 repeat units have been prepared and spectroscopically characterized. The porphyrin-bridged Pd complex has been used for the stabilization of gold nanoparticles, thus giving rise to unexpected stable structures with no evidence of covalent bonds between the porphyrin and the gold nanoparticles. The morphology investigated by TEM analysis shows that gold nanoparticles with a mean diameter of about 5 nm have been obtained. UV/Vis spectra reveal the achievement of stabilized gold nanoparticles through the presence of the plasmon resonance at 500 nm together with the absorption features of the porphyrin molecule at 436 and 620 nm (Q band). Photoluminescence spectra exhibit an emission feature centred at 572 nm with a shoulder at 325 nm with no quenching effects. XPS measurements at the Au 4f core level suggest an electronic interaction between the gold atoms of the nanoparticle surface and the porphyrin-based complex; NMR spectroscopic studies indicate that interactions and assemblies also occur that involve the porphyrin rings. Elemental analysis suggests that about 120 tilted porphyrins are physisorbed onto the Au core.

Introduction

Porphyrins are a class of multifunctional and versatile π-conjugated molecules with interesting optical, photocatalytic and light-harvesting properties that have shown great potential in the fabrication of multifunctional electronic and optical devices through covalent linking to metal nanoparticles.[1–3] Understanding the factors that affect the interaction between chromophores and metal nanoparticles is essential in the design of effective applications. The rational design of gold nanoparticles that link different stabilizers has driven extended studies because these complex structures offer the chance to bind and incorporate various organic, inorganic or bioactive molecules.[4,5] Recently Pd^{II}-containing organometallic thiols have also been used for the stabilization of gold nanoparticles (AuNPs).[6]

In the case of porphyrin-functionalized gold nanoparticles, energy-transfer processes from the photoexcited chromophore to the gold core lead to quenching of porphyrin fluorescence in porphyrin-functionalized gold nanoparticles.[7] Porphyrins as linkers on gold nanoparticles also have the advantage of exploiting multiple binding sites to achieve a better control of the orientation of porphyrins on the gold core.[8] Free-base porphyrins with two thioacetate-terminated linkers in different positions on the porphyrin molecule have been used for the stabilization of gold nanoparticles and short fluorescence lifetimes have been measured, thus indicating efficient energy transfer to the gold cores.[9] The control of the size of gold nanoparticles is also an important feature; it has been achieved by the link of a tetradentate porphyrin monolayer on the gold surface with well-defined orientation,[10] and gold nanoparticles stabilized with porphyrins with four sulfur atoms provide quite small size-controlled gold nanoparticles.[11,12] The tuning of the plasmon coupling between the Au nanocrystals of linear chains of Au nanorods is proposed for tetrakis(4-sulfonatophenyl)porphyrin aggregates in solution, thereby providing potential applications of metal nanocrystals in the areas of photonics, electronics and optics.[13] The transduction of optical radiation to current in a molecular circuit made by a network array of AuNPs bridged through a dithiol–Zn porphyrin trimer has been recently reported, which suggests that the plasmon-controlled electrical properties of these molecules can be tailored to be applied in optoelectronic and energy-harvesting devices.[14] Gold nanoparticles are usually stabilized by a sulfur–Au covalent bond, and a few examples of physisorption of a porphyrin derivative without covalent bonding are known.[15] The assembly of gold nanoparticles stabilized by noncovalently bonded electro-optically active conjugated molecules is a suitable model to study the electronic structure of the molecules that interact with gold nanoparticles.

In this paper we report the synthesis and characterization of a Zn–porphyrin-bridged diacetylide Pd^{II} complex with

[a] Department of Chemistry, "Sapienza" University of Rome, P.le A. Moro 5, Box 34 Roma 62, 00185 Rome, Italy
E-mail: ilaria.fratoddi@uniroma1.it
[b] Department of Physics, unità INSTM and CISDiC University Roma Tre, Via della Vasca Navale 85, 00146 Rome, Italy
[c] Università Telematica Internazionale UniNettuno, Facoltà di Ingegneria Corso Vittorio Emanuele II, 39 00186, Rome, Italy

Supporting information for this article is available on the WWW under http://dx.doi.org/10.1002/ejic.201100339.

extended π conjugation capable of efficiently interacting with gold nanoparticles by physisorption to yield stable conjugates without the need for S–Au bonding.

Results and Discussion

Synthesis and Characterization of Pd–Porphyrin Complex 4 and Oligomer 5

The synthetic route to yield the porphyrin-bridged Pd complexes is based on the widely applicable dehydrohalogenation reaction.[16] This reaction was successfully used for the achievement of porphyrin-bridged Pt complexes and oligomers, the chemical and electronic structure of which has been investigated in depth in our group.[17–19] These multinuclear Pt complexes are also capable of self-assembly into nanostructured features.[20] However, the synthesis of analogous Pd complexes proved to be very difficult, because of decomposition that occurs during purification (crystallization and chromatography). Previous attempts to prepare complex **4** gave preliminary results and few insights into the self-assembly properties of this complex in comparison with the Pt analogues studied.[21] The synthesis has now been reinvestigated, and the products carefully characterized. The reaction routes that started from Zn–porphyrin **1** and led to complexes **4** and **5** are depicted in Scheme 1.

The reaction courses were monitored with UV/Vis absorption measurements at subsequent times; the intensity of the Soret band at 424 nm of precursor **1** decreased, whereas those of the bands at 452 nm for complex **4** and 462 nm for oligomer **5** increased. Oligomer **5** showed a moderate increase in electron delocalization through the macromolecule, with a considerable redshift in the band relative to that of ZnDEP. The FTIR spectra of **4** and **5** confirm the achievement of the coupling reaction by the absence of the band at 3200 (free NH in non-metalated porphyrin) and of the bands at 3264 and 622 cm^{-1} characteristic of the H–C≡C stretching mode and bending mode, respectively, of **1**, whereas enhancement of intensity and a slight shift in the band for the C≡C stretching mode [2083 cm^{-1} for **1**, 2079 cm^{-1} for complex **4** and 2066 cm^{-1} for complex **5**, respectively] were found.

The full characterization of **4** was accomplished by means of NMR spectroscopic investigations. The ^1H 1D NMR and COSY spectra of **4** can roughly be divided into two regions; the first one ranges from about δ = 0.60 ppm to about 5.00 ppm in which aliphatic protons resonate, whereas in the latter region (from δ = 7 to 10 ppm) aromatic protons can be observed. The COSY spectrum allowed us to unequivocally assign all proton resonances; experimental details are reported in the Supporting Information. The ^{31}P NMR spectrum evidenced a single resonance at δ = 10.86 ppm for the two equivalent phosphane ligands. The observed resonances confirmed the structure of complex **4**. The ^1H NMR spectrum of **5** shows the characteristic complexity of polydispersed species, yet it was possible to recognize the polymer resonances by comparison with the spectrum of **4**. The ^{31}P NMR spectrum shows two resonances

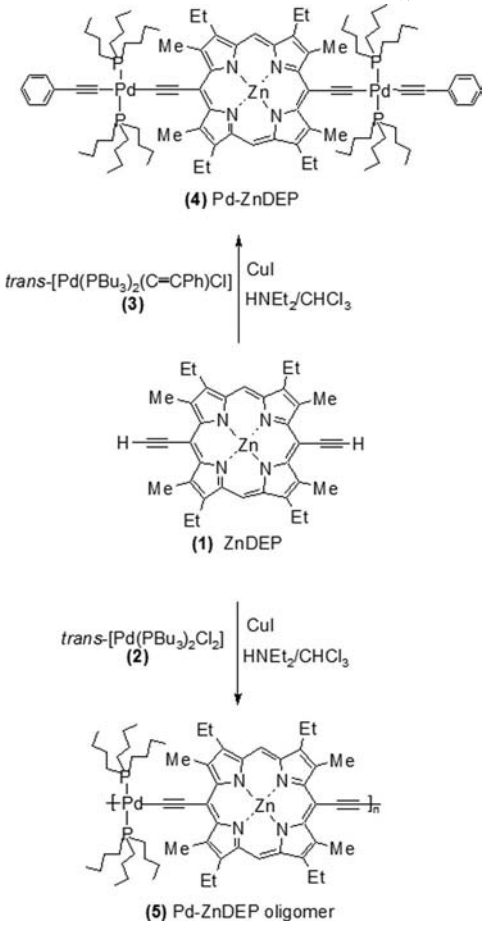

Scheme 1. Reaction scheme and chemical structures of ZnDEP (**1**), complex **4** and oligomer **5**.

at δ = 10.46 and 11.60 ppm, which are attributed to phosphorus atoms on terminal and internal sites, respectively.[16] The relative integrals are about 1:1.5 (i.e. corresponding to an oligomer made of 3–5 units). A GPC analysis was carried out and M_w and M_n data (M_w=5570 a.m.u., M_n=3700 a.m.u.) agree with the ^{31}P NMR spectroscopic results.

NOESY spectra with several mixing times (150, 200, 250 and 500 ms) were acquired with the aim of exploring the molecule spatial arrangement of complex **4**. Strong dipolar correlations, which correspond to interproton distances that range from 2 to 3 Å, were observed among the *n*-butyl protons and between the $–CH_3$ protons and the *n*-butyl ones. Smaller cross peaks, which correspond to interproton distances that range from 3 to 5 Å, were observed between the resonance of *ortho* aromatic protons and *n*-butyl protons and between *meso* protons and $–CH_2$ ethyl protons. Those correlations suggest that some *n*-butyl chains could be positioned near the porphyrin ring and others near the phenyl groups. To evaluate the possibility of intermolecular stacking, several 1D proton and 2D NOESY experiments were acquired with a concentration that ranged from 0.5 mg/0.6 mL to 2 mg/0.6 mL according to previous studies.[22] In this concentration range, no chemical shift, half-height

Table 1. XPS data collected on complex **4** and oligomer **5**; the same data collected and already published for the *trans*-[$Pd(PBu_3)_2Cl_2$] complex are also reported for comparison.

Sample	C 1s E_B (fwhm) [eV]	Pd $3d_{5/2}$ E_B (fwhm) [eV]	P $2p_{3/2}$ E_B (fwhm) [eV]	Zn $2p_{3/2}$ E_B (fwhm) [eV]	N 1s E_B (fwhm) [eV]
4	283.40	337.70	130.75	1022.00	398.24
	284.70	(1.78)	(1.65)	(1.65)	(1.65)
	(1.76)				
5	283.20	337.83	130.86	1022.20	398.26
	284.70	(1.77)	(1.55)	(3.2)	(1.64)
	(2.16)				
trans-[$PdCl_2(PBu_3)_2$]	285.00	338.07	130.90	–	–
	(1.50)	(1.42)	(1.42)		

width or dipolar correlation variations were observed, thus suggesting that the molecule does not show auto-assembly behaviour. The half-height width variations provide the relationship between this parameter and transversal relaxation time T_2;[23] thus by comparing two peaks with different widths, the broader resonance can be assigned to the molecular moiety that rotates more slowly. The absence of half-height width variations for the resonance of the *meso* protons is very important since a broadening of their line shape is indicative of an interaction that involves the porphyrin ring. Since this behaviour is common for all proton resonances, this is a further indication that the molecule does not auto-assemble in the examined concentration range, as reported in the literature in analogous studies on porphyrin materials.[24]

The binuclear complex **4** and compound **5** were investigated by means of X-ray photoelectron spectroscopy with the aim of investigating both the electronic and molecular structure. C 1s, Pd 3d, P 2p, Cl 2p, Zn 2p and N 1s signals were collected and analyzed, as reported in Table 1. The collected data were compared to the ones measured for the *trans*-[$Pd(PBu_3)_2Cl_2$] precursor to investigate the expected electronic structure modifications. A Pd $3d_{5/2}$ signal was found at a binding energy (E_B) of 337.70 eV in both porphyrin complex **4** and compound **5**, only slightly shifted from that of the precursor that is at E_B = 338.07 eV, which suggests slight electron conjugation through the π-conjugated organic moieties and the metal centre. The 0.37 eV E_B shift is clearly shown in Figure 1, in which the Pd 3d spectra of the three samples are displayed.

The C 1s signals of both complex **4** and compound **5** show two main components. The component at 284.70 eV is due to aliphatic and (most) aromatic C atoms; the less intense component at E_B = 283.40 eV is attributed to C atoms bonded to the metal centre, as already reported in the literature for organometallic compounds.[16] N 1s signals appear at about E_B = 398.26 eV for both samples, as expected for N atoms of the metalloporphyrin ring.[21]

The Cl 2p core level was carefully analyzed for compound **5**, with the aim of individuating the terminal groups and estimating the number of repetitive units. A Cl $2p_{3/2}$ signal at E_B = 198.05 was detected, as expected for chlorine terminal groups in organometallic compounds.[25] From the Cl 2p/Pd 3d signal ratio a chain length of 3–4 metal units was calculated, as also suggested by the GPC and ^{31}P NMR spectroscopic results.

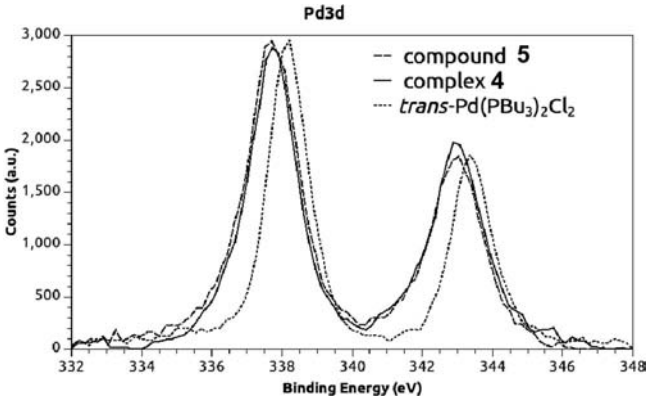

Figure 1. Pd 3d spectra of complex **4** and oligomer **5**. The same spectrum measured for [$Pd(PBu_3)_2Cl_2$] is superimposed for comparison.

Synthesis and Characterization of Porphirin-Stabilized Gold Nanoparticles (AuNPs-4)

Gold nanoparticles coated with complex **4** were prepared by $NaBH_4$ reduction of $HAuCl_4$ in a two-phase procedure to give red porphyrin-stabilized gold nanoparticles AuNPs-**4**. Gold nanoparticles AuNPs-**4** were stable and the surface plasmon band did not change over weeks. Figure 2 shows the UV/Vis absorption and emission (photoluminescence, PL) spectra of the purified AuNPs-**4** nanoparticles in comparison with those of complex **4**. The spectrum shows both features characteristic of the porphyrin and gold nanoparticles (i.e. the Soret and Q bands at 436 and 620 nm, respectively, and the surface plasmon band at around 500 nm). The Soret band of AuNPs-**4** was significantly broadened and blueshifted relative to that of **4** before reduction: 436 nm for AuNPs-**4** versus 452 nm for **4** were detected, thereby suggesting that electronic interactions between gold nanoparticles and the porphyrin and/or side-by-side alignment of **4** on the gold surface occur.[26] Moreover, a ligand-dependent decrease of the Soret-band intensity is observed

that also points to an electronic interaction between the porphyrin and the Au nanoparticles.[27] The PL spectra show an emission peak at about 572 nm with a shoulder at 625 nm and no quenching effects and features significantly narrower and blueshifted bands relative to those of complex **4** ($\Delta\lambda$ = 67 nm). By considering that porphyrins very close to each other and to the gold nanoparticle surface show a broadening in the absorption features because of aggregation effects,[28] the optical results confirm an interaction between the Au core and the porphyrin ligand.

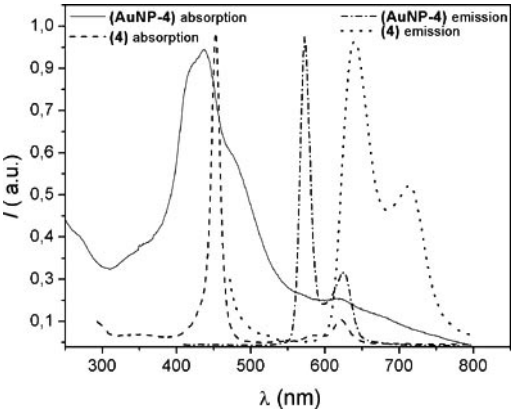

Figure 2. UV absorption and emission spectra of **4** and AuNPs-**4** in $CHCl_3$.

Figure 3 shows a TEM image of AuNPs-**4**. The particle distribution consists of two populations; the mean diameter of the observed spherical particles is 5.0 ± 1.4 nm and contains roughly 2000 gold atoms, calculated according to a literature report[29] with a surface area of about 50 nm^2. By considering the elemental analysis results,[30] a single gold nanoparticle should interact with approximately 120 molecules of complex **4**; the ratio between the number of gold atoms and the number of complex **4** molecules is equal to 16.7. In analogy to what was reported in the literature for *meso*-5,10,15,20-tetrakis-2-thienylporphyrin physisorbed onto gold nanoparticles and by using the cross-sectional area of a similar compound that can be adsorbed onto gold nanoparticles in flat or edge-on configurations (approximately 1.7 and 0.8 nm^2),[15] we can assume that 120 molecules of complex **4** are arranged on the gold surface with a tilted conformation (see Figure 3b) and in which porphyrin rings interact with each other, as reported for similar porphyrin complexes adsorbed onto flat gold surfaces.[21,31]

The 1D proton spectra of AuNPs-**4** nanoparticles were acquired and are reported in Figure 4 together with the ^1H NMR spectrum of complex **4**. The spectral profile of AuNPs-**4** is similar yet different to the one observed for the isolated molecule. As before, the spectrum can be divided into an aliphatic region between δ = 0.50 and 4.00 ppm, an aromatic region between δ = 6.8 and 7.5 ppm and the *meso* proton region at about δ = 10 ppm. In the region between δ = 0.70 and 2.00 ppm several complex resonances can be observed: a broad signal at δ = 0.77 ppm, a multiplet at δ = 0.89 ppm and another broad resonance from 1.20 to

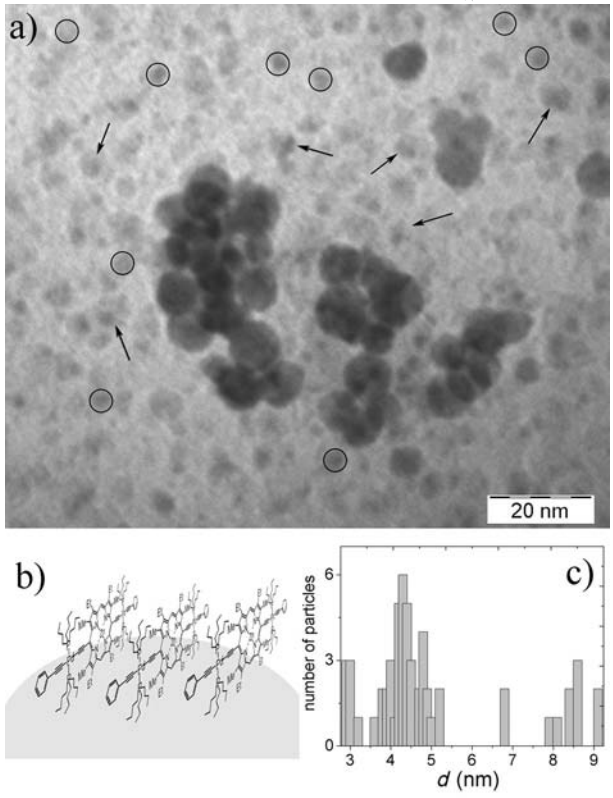

Figure 3. (a) TEM images of AuNPs-**4** with mean diameter (5.0 ± 1.4) nm, circles have been added to easily distinguish some of the many particles with low sizes; the arrows indicate small particles characterized by some shape and faceting. (b) Tilted conformation model of complex **4** on the gold surface. (c) Dimensions distribution.

1.63 ppm superimposed with the water singlet at δ = 1.47 ppm. In this region the resonances due to the *n*-butyl CH_3 and CH_2 protons and several broad multiplets at δ = 1.72 and 1.88 ppm, respectively, assigned to terminal CH_3 protons of the ethyl groups on the porphyrinic ring are observed. Between δ = 3.30 and 4.00 ppm broad resonances can be observed at δ = 3.64 and 3.94 ppm, which are associ-

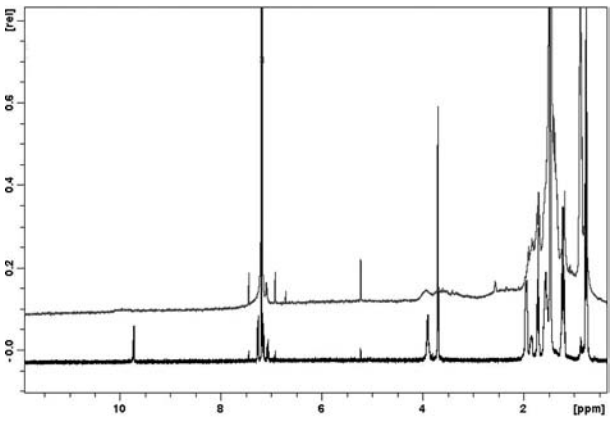

Figure 4. ^1H NMR spectra of complex **4** (black) and AuNPs-**4** (grey).

Table 2. XPS data (E_B, fwhm) collected on sample AuNPs-**4**. For comparison, complex **4** XPS data are also reported.

Sample	C 1s E_B (fwhm) [eV]	Pd $3d_{5/2}$ E_B (fwhm) [eV]	P $2p_{3/2}$ E_B (fwhm) [eV]	Zn $2p_{3/2}$ E_B (fwhm) [eV]	N 1s E_B (fwhm) [eV]	Au $4f_{7/2}$ E_B (fwhm) [eV]
4	284.70 (1.76)	337.70 (1.78)	130.75 (1.65)	1022.00 (1.65)	398.24 (1.65)	–
AuNPs-**4**	284.70 (1.96)	338.36 (1.83)	130.81 (1.62)	1021.66 (2.10)	398.41 (2.15)	83.56 84.98 (1.52)

ated to CH_2 and methyl groups on the porphyrinic ring. In the aromatic region a broad, complex resonance is found between δ = 7.06 and 7.40 ppm. The signal at δ = 7.06 ppm is attributed to the aromatic *para* protons of the terminal phenyl ring, the deformed doublet at δ = 7.16 ppm to the *meta* protons and the other doublet at δ = 7.27 ppm to the *ortho* protons. At lower fields, a broad singlet at δ = 9.94 ppm can be identified and attributed to the *meso* protons.

The spectrum of AuNPs-**4** differs from that acquired for the isolated molecule, slight chemical-shift variations and, more importantly, a general broadening of all resonances. For example, the terminal *n*-butyl CH_3 in **4** shows a width of 1.48 Hz, which increases to about 4 Hz in the case of the nanoparticles. A similar resonance broadening can be observed for all the molecule protons with a various degree of broadening; noteworthy is that the CH_2 signal of the ethyl group widens from 4.5 to 70.5 Hz; the *meso* proton singlet is the most affected, thereby increasing its width from 1.5 to about 130 Hz. This significant increase in the half-height width, which corresponds to a much longer correlation time relative to that of the isolated molecule and thus to a lower mobility, strongly suggests the formation of an interaction between complex **4** molecules in AuNPs-**4**.[32] Since the greater half-height width variation is observed for the resonance of the *meso* protons, and by considering that their chemical shift is also the most affected by the interaction with Au, it could be hypothesized that complex **4** stabilizes the nanoparticles through the porphyrinic rings yet still retains a degree of mobility for the *n*-butyl and phenyl moieties.

X-ray photoelectron spectroscopy measurements were also performed on the porphyrin-stabilized gold nanoparticles AuNPs-**4**; data were acquired at C 1s, N 1s, P 2p, Pd 3d, Zn 2p and Au 4f core-energy levels and compared to the data acquired on pristine complex **4**, as shown in Table 2.

The C 1s, N 1s, Pd 3d, Zn 2p and P 2p E_B values observed for the AuNPs-**4** sample are quite close to those measured for complex **4**, thus showing that the interaction with gold nanoclusters does not affect the chemical structure of the Zn–porphyrin complex.

The Au 4f spectrum is reported in Figure 5; by following a curve-fitting procedure, two contributions to the two spin–orbit components are detected. The Au $4f_{7/2}$ component of the peak at lower E_B values (83.69 eV) is due to metallic gold; the second Au $4f_{7/2}$ component at E_B = 84.98 eV can been associated to the Au atoms that interact with the organometallic molecule. XPS data support a physisorption occurring between the gold nanoparticles and the porphyrin-based complex with no significant E_B shifts in the core-level spectra of complex **4** atoms.

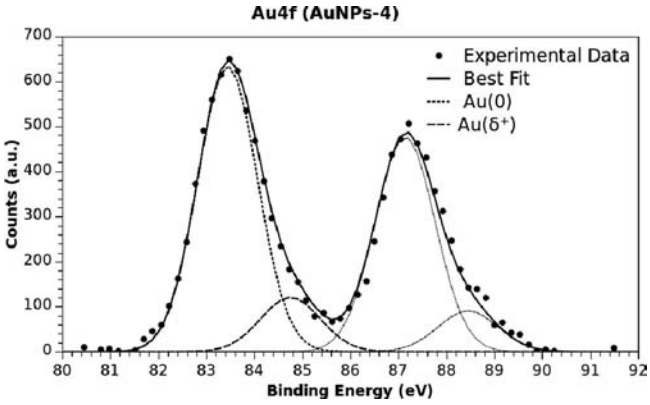

Figure 5. XPS Au 4f spectrum of AuNPs-**4**.

Conclusion

Protected gold nanoparticles have been prepared with a porphyrin-bridged di-bis(tributylphosphane)palladium–diphenylacetylide dinuclear complex **4** as stabilizing agent. The analogous oligomer with 3–5 repeat units (**5**) has also been prepared and spectroscopically characterized. The gold nanoparticles surrounded by the porphyrin complex (AuNPs-**4**) show a spherical shape with mean diameter of about 5 nm, observed by TEM analysis. The optical characterizations allowed us to assess the plasmon resonance at 500 nm and the absorption features of the porphyrin-based complex at about 440 and 620 nm; also, no quenching effects in the emission features centred at 572 nm with a shoulder at 325 nm have been observed. NMR spectroscopy, XPS and elemental analyses suggest the unusual assembly of about 120 densely packed physisorbed porphyrin-based complex molecules tilted on the Au core, with no evidence of covalent bonds between the porphyrin and the gold nanoparticles. This study suggests promising applications of gold–porphyrin hybrids in an unconventional assembly for the development of future optoelectronic devices.

Experimental Section

Materials: Deionized water was obtained from a Millipore Milli-Q water purification system. Hydrogen tetrachloroaurate(III) trihydr-

ate (Aldrich, 99.9+%), tetraoctylammonium bromide (Aldrich, 98%), sodium borohydride (Aldrich, 99%), sodium sulfate anhydrous (Carlo Erba), Celite 545 filter agent (Aldrich) and florisil were used as received. All solvents (Aldrich, reagent grade) were dried with Na_2SO_4 before use. Argon was passed through the reaction solvents to deoxygenate the reaction systems, the reactions were further performed under an argon atmosphere by using standard labware.

2,8,12,18-Tetraethyl-5,15-diethynyl-3,7,13,17-tetramethylporphyrinatozinc(II) (**1**; ZnDEP) was synthesized according to a literature report[33] from 3,7,13,17-tetraethyl-2,8,12,18-tetramethyl-10,20-bis(trimethylsilylethynyl)pophyrin (ZnDEPSi) (**1a**)[34] and precursor dichloride and monochloro acetylide Pd^{II} complexes {i.e. *trans*-[$Pd(PBu_3)_2Cl_2$] (**2**) and *trans*-[$Pd(PBu_3)_2(C{\equiv}C{-}C_6H_5)Cl$] (**3**)} obtained by means of already published methods.[35,36] Spectral data are reported in the Supporting Information.

Methods: FTIR spectra were recorded as films deposited from $CHCl_3$ solutions by using ZSM-5 cells with a Bruker Vertex 70 Fourier transform spectrometer. ^1H and ^{31}P NMR spectra were recorded with a Bruker AC 300P spectrometer at 300 and 121 MHz, respectively, in $CDCl_3$; the chemical shifts (ppm) were referenced to TMS for ^1H NMR spectra by assigning the residual ^1H impurity signal in the solvent at δ = 7.24 ppm ($CDCl_3$). ^{31}P NMR spectroscopic chemical shifts are relative to H_3PO_4 (85%). UV/Vis spectra were recorded with a Varian Cary 100 instrument. Photoluminescence spectra were performed with a Perkin–Elmer LS 50 fluorescence spectrometer. All optical measurements were performed at room temperature in $CHCl_3$. Elemental analyses were provided by the Servizio di Microanalisi of the Department of Chemistry with an EA 1110 CHNS-O instrument. Number-average molecular weight (M_n), weight-average molecular weight (M_w) and dispersity Đ = M_w/M_n[37] were determined by gel permeation chromatography (GPC) on a PL-gel column that contained a highly cross-linked spherical polystyrene/divinylbenzene matrix packed with 10 micron particles with a pore size of 100 Å. $CHCl_3$ (HPLC grade) was used as eluent and pumped at a flow rate of 0.8 mL min^{-1} by a binary LC pump through an injection loop with a volume of 24 μL. Monodisperse polystyrene standards were used for calibration, and the samples detected with a UV detector. Mass spectra were acquired with a Bruker MicroToF mass spectrometer. For transmission electron microscopy (TEM) observations and the diffraction contrast imaging, a FEI TECNAI G2 F30 Supertwin field-emission gun scanning transmission electron microscope (FEG STEM) operating at 300 kV and with a point-to-point resolution of 0.205 nm was used. The TEM specimens were prepared by depositing a few drops of the diluted solutions on carbon-coated TEM grids to be directly observed in the instrument. XPS analysis was performed with an instrument of our own design and construction. It consisted of a preparation and an analysis UHV chamber equipped with a 150-mm mean radius hemispherical electron analyzer with a four-element lens system with a 16-channel detector, thus giving a total instrumental resolution of 1.0 eV as measured at the Ag $3d_{5/2}$ core level. Mg-K_α non-monochromatized X-ray radiation ($h\nu$ = 1253.6 eV) was used for acquiring core-level spectra of all samples (C 1s, N 1s, P 2p, Pd 3d, Zn 2p and Au 4f). The spectra were energy referenced to the C 1s signal of aromatic C atoms with a binding energy E_B = 284.70 eV. Atomic ratios were calculated from peak intensities by using Scofield's cross-section values and calculated λ factors.[38] Curve-fitting analysis of the C 1s, N 1s, P 2p, Pd 3d, Zn 2p and Au 4f spectra was performed by using Voigt profiles as fitting functions after subtraction of a Shirley-type background.[39] All NMR spectra were carried out with a Bruker Avance 400 spectrometer operating at a frequency of 400.13 MHz for the proton in $CDCl_3$ with TMS as chemical-shift reference. Monodimensional proton spectra were acquired at a temperature of 298 K by employing the sequence present in the spectrometer routines with a spectral width of 15 ppm, 64000 data points, an acquisition time of 5.5 s, a repetition time of 5 s and 16 scans. Bidimensional COSY experiments[40] were recorded at 298 K by employing the sequence present in the spectrometer routines. Bidimensional homonuclear proton NOESY[41,42] experiments were acquired with several mixing times (150, 200, 250 and 500 ms) at 298 K by employing the sequences present in the spectrometer routines. All homonuclear bidimensional spectra were acquired with a spectral width of 15 ppm in both dimensions, a matrix of $2k \times 512$ data points for both the direct and the indirect dimensions, a repetition delay of 2 s and 64 scans. All spectra were processed with Bruker Topspin 1.3 software.

General Procedures: The Pd–ZnDEP binuclear complex **4** and the polynuclear compound **5** have been synthesized by condensation of **1** with *trans*-[$Pd(PBu_3)_2Cl_2$] or *trans*-[$Pd(PBu_3)_2(C{\equiv}C{-}C_6H_5)Cl$], respectively, by a procedure modified from that reported for the synthesis of multinuclear Pt analogous compounds (method a);[43] compound **4** was obtained with a "one-pot" method as well (method b). The reaction scheme and the chemical structures are reported in Scheme 1.

Synthesis of Porphyrin-Bridged Di-bis(tributylphosphane)palladium Diphenylacetylide (4): Method a: In a 150-mL three-necked flask, [$Pd(PBu_3)_2(C{\equiv}C{-}C_6H_5)Cl$] (**3**, 123 mg, 0.197 mmol) was dissolved in a mixture of solvents [30 mL of $NHEt_2/CHCl_3$ (2:1 v/v), previously degassed with argon flux for 30 min]. CuI (2 mg) was added at T = 25 °C to the thoroughly stirred mixture. A solution (30 mL) of ZnDEP (**1**, 46.7 mg, 0.079 mmol) in $NHEt_2/CHCl_3$ (2:1 v/v) was then added dropwise to the previous mixture over 45 min in the dark. The reaction course was monitored by UV/Vis spectroscopy until a strong absorption band at 452 nm was detected after 3 h. The reaction was interrupted by immersing the flask in an ice/salt bath, and the mixture was dried in vacuo to obtain a solid crude product. The crude mixture was washed thoroughly with water three times to eliminate the ammonium salt side product, and the organic phase was concentrated to small volume with a rotavapor and dried with anhydrous Na_2SO_4. MeOH was added to this small volume (about 5 mL) and left at T = 4 °C to yield the purified product (**4**). Yield: 36 mg (0.020 mmol, 25%). ^1H NMR ($CDCl_3$): δ = 0.76 (t, J = 7.15 Hz, $PCH_2CH_2CH_2CH_3$), 1.22 (m, J = 7.15, 7.50 Hz, $PCH_2CH_2CH_2CH_3$), 1.56 (m, J = 7.50, 4.40 Hz, $PCH_2CH_2CH_2CH_3$), 1.71 (t, J = 7.75 Hz, CH_2CH_3), 1.95 (m, $PCH_2CH_2CH_2CH_3$), 3.70 (s, CH_3), 3.89 (q, J = 7.75 Hz, CH_2CH_3), 7.16 (d, 2 H, *para*-phenyl), 7.27 (d, 4 H, *ortho*-phenyl), 7.37 (t, 4 H, *meta*-phenyl), 9.72 (s, *meso*-2 H) ppm. ^{31}P NMR ($CDCl_3$): δ = 10.86 ppm. UV/Vis ($CHCl_3$): λ_{max} = 277, 452, 588, 620 nm. FTIR (nujol): $\tilde{\nu}$ = 2079 [ν(C≡C)], 1597 [ν(C=C), arom.], 1208 [ν(C–H), pyrrole], 845 [ν(C–N), pyrrole] cm^{-1}. $C_{100}H_{152}P_4N_4Pd_2Zn$: calcd. C 66.27, H 8.45, N 3.09; found C 64.80, H 8.04, N 3.38. MS: m/z = 1812.4 (molecular peak).

Method b: In a three-necked flask, 3,7,13,17-tetraethyl-2,8,12,18-tetramethyl-10,20-bis(trimethylsilylethynyl)pophyrin (DEPSI; 35.8 mg, 0.053 mmol) was dissolved in THF (10 mL) with tetrabutylammonuim bromide (100 μL) whilst stirring in the dark at T = 25 °C for 1 h. In another three- necked vessel, a solution made from [$Pd(PBu_3)_2(C{\equiv}C{-}C_6H_5)Cl$] (69.1 mg, 1.11 mmol) and CuI (1 mg) dissolved in an $NHEt_2/CHCl_3$ mixture (20 mL, 1:1 v/v) was prepared. After 1 h, $NHEt_2$ (10 mL) was poured into the first reaction flask, and, while increasing the pressure of argon, this reaction mixture was added dropwise into the second one over 3.5 h. Also in

this case, the reaction course was monitored by UV/Vis spectroscopy until a strong absorption band at 452 nm was detected. The resulting reaction solution was handled as reported for method a. The final small-volume organic solution was purified by elution with THF on a short column for chromatography (florisil). The eluted material was further purified by crystallization (THF/MeOH), and pure complex **4** was obtained. Yield: 29.6 mg (0.017 mmol, 32%). The elemental analysis and spectroscopic characterizations are consistent with those reported in method a.

Synthesis of Porphyrin-Bridged Oligomer (5): ZnDEP (**1**) (200 mg, 0.30 mmol), $[Pd(PBu_3)_2Cl_2]$ (175 mg, 0.21 mmol) and CuI (3.5 mg) were mixed in a three-necked reaction vessel with the solvent mixture $NHEt_2/CHCl_3$ (60 mL, 1:1 v/v) whilst stirring in the dark at T = 25 °C for 3 h. A shift in the absorption band was observed from 430 (Soret band of ZnDEP) to 462 nm (end of the reaction). The reaction solution was submitted to the same purification procedure reported for method b. Yield: 150 mg (40 wt.-%). ^{1}H NMR ($CDCl_3$): δ = 1.70 (t, 12 H, CH_2CH_3), 2.95 (s, 12 H, CH_3), 3.69 (s, 6 H, OCH_3), 3.82 (q, 8 H, CH_2CH_3), 6.17 (dd, 4 H, C≡C–$C_6H_4OCH_3$), 6.47 (dd, 4 H, C≡C–$C_6H_4OCH_3$), 7.84–7.08 (m, 60 H, P–C_6H_5), 9.66 (s, *meso* 2 H) ppm. ^{31}P NMR ($CDCl_3$): δ = 10.46 (terminal), 11.60 ppm (internal), integral ratio 1:1.5. UV/Vis ($CHCl_3$): λ_{max} = 462, 495, 593, 632, 705 nm. FTIR (nujol): $\tilde{\nu}$ = 2066 [ν(C≡C)], 1596 [ν(C=C), arom.], 1250 [ν(C–H), pyrrole], 856 [ν(C–N), pyrrole], 446, 400 [ν(Pd–P)] cm^{-1}. $C_{56}H_{85}N_4P_2PdZn$ (repeat unit) (%): calcd. C 65.56, H 8.07, N 5.00; found C 63.48, H 7.80, N 5.10. GPC: M_w 5570, M_n 3700 a.m.u., Đ = 1.5 (repeat unit 1048 a.m.u., then the oligomer is made by 3–5 units).

Synthesis of Pd–porphyrin-Stabilized Gold Nanoparticles (AuNPs-4): The porphyrin-stabilized gold nanoparticles were prepared at room temperature (r.t.) in a two-phase system by following an assessed procedure.[44,45] The molar ratio of Au/porphyrin was 1:1. Compound **4** (50.0 mg, 0.0286 mmol) was dissolved in dichloromethane (20 mL) and added to a 0.03 M solution of $HAuCl_4 \cdot H_2O$ (1.00 mL) in deionized water (11.3 mg, 0.0286 mmol). Tetraoctylammonium bromide (TOAB; 20.0 mg) was added and then a 0.05 M aqueous solution of $NaBH_4$ (10 mL, 20.0 mg, 0.529 mmol) was poured into it dropwise under vigorous stirring. The reaction mixture was allowed to react for 3 h at room temperature. Extraction with H_2O/CH_2Cl_2 followed. The obtained green–brown solid was isolated by evaporation of the organic layer. The solid was re-suspended in methanol, washed with acetonitrile and hexane, recovered from dichloromethane and dried for 3 d under vacuum. Yield: 15 wt.-%. The UV/Vis spectra of the washing solutions showed the absence of plasmon absorption arising from AuNPs and a low absorption from the free porphyrin (Soret band: 452 nm). UV/Vis ($CHCl_3$): λ_{max} = 436, 500, 590, 620 nm. FTIR (film): $\tilde{\nu}$ = 2932, 2871, 2084 [ν(C≡C)], 1600 [ν(C=C), arom.], 1468, 1454, 1354, 1055, 852 [ν(C–N), pyrrole], 446 [ν(Pd–P)] cm^{-1}. Elemental analysis: found C 22.82, H 4.12, N 0.36.

Supporting Information (see footnote on the first page of this article): Experimental details, UV-Vis, ^{1}H NMR, ^{31}P NMR, IR, PL, COSY and NOESY spectra and data of the compounds are presented.

Acknowledgments

The authors gratefully acknowledge the financial support to this research by Progetti Ateneo Sapienza 2009 (C26A09AS5R), Ateneo Federato AST 2008 (26F09MA27) and the MAE-Ministero dell'Università e della Ricerca (MIUR), Progetti di Ricerca Scientifica e Tecnologica Bilaterale 2008–2010. The authors would like to thank Prof. Marco Rossi and Dr. Roberto Matassa for helpful comments and discussion of the TEM analysis.

[1] S. Fukuzumi, *Eur. J. Inorg. Chem.* **2008**, *9*, 1351–1362.
[2] Y. Kobuke, *Eur. J. Inorg. Chem.* **2006**, *12*, 2333–2351.
[3] M. Drobizhev, Y. Stepanenko, A. Rebane, C. J. Wilson, T. E. O. Screen, H. L. Anderson, *J. Am. Chem. Soc.* **2006**, *128*, 12432–12433.
[4] J.-S. Lee, J. J. Green, K. T. Love, J. Sunshine, R. Langer, D. G. Anderson, *Nano Lett.* **2009**, *9*, 2402–2406.
[5] S. I. Lim, C. J. Zhong, *Acc. Chem. Res.* **2009**, *42*, 798–808.
[6] F. Vitale, R. Vitaliano, C. Battocchio, I. Fratoddi, C. Giannini, E. Piscopiello, A. Guagliardi, A. Cervellino, G. Polzonetti, M. V. Russo, L. Tapfer, *Nanoscale Res. Lett.* **2008**, *3*, 461–467.
[7] H. Imahori, M. Arimura, T. Hanada, Y. Nishimura, I. Yamazaki, Y. Sakata, S. Fukuzumi, *J. Am. Chem. Soc.* **2001**, *123*, 335–336.
[8] T. Hasobe, *Phys. Chem. Chem. Phys.* **2010**, *12*, 44–57.
[9] A. Kotiaho, R. Lahtinen, A. Efimov, H. Lehtivuori, N. V. Tkachenko, T. Kanerva, H. Lemmetyien, *J. Photochem. Photobiol. A: Chem.* **2010**, *212*, 129–134.
[10] J. Ohyama, Y. Hitomi, Y. Higuchi, M. Shinagawa, H. Mukai, M. Kodera, K. Teramura, T. Shishido, T. Tanaka, *Chem. Commun.* **2008**, 6300–6302.
[11] J. Ohyama, Y. Hitomi, Y. Higuchi, T. Tanaka, *Top. Catal.* **2009**, *52*, 852–859.
[12] A. Satake, M. Fujita, Y. Kurimoto, Y. Kobuke, *Chem. Commun.* **2009**, 1231–1233.
[13] L. Zhang, H. Chen, J. Wang, Y. F. Li, J. Wang, Y. Sang, S. J. Xiao, L. Zhan, C. Z. Huang, *Small* **2010**, *6*, 2001–2009.
[14] P. Banerjee, D. Conklin, S. Nanayakkara, T.-H. Park, M. J. Therien, D. A. Bonnell, *ACS Nano* **2010**, *4*, 1019–1025.
[15] Y. Noda, S. Noro, T. Akutagawa, T. Nakamura, *Phys. Rev. B* **2010**, *82*, 205420.
[16] I. Fratoddi, C. Battocchio, A. La Groia, M. V. Russo, *J. Polym. Sci., Part A Polym. Chem.* **2007**, *45*, 3311–3329.
[17] I. Fratoddi, C. Battocchio, R. D'Amato, G. P. Di Egidio, L. Ugo, G. Polzonetti, M. V. Russo, *Mater. Sci. Eng. C: Biom. Supramol. Syst.* **2003**, *C23*, 867–871.
[18] C. Battocchio, I. Fratoddi, M. V. Russo, G. Polzonetti, *J. Phys. Chem. A* **2008**, *112*, 7365–7373.
[19] C. Battocchio, I. Fratoddi, R. Vitaliano, M. V. Russo, G. Polzonetti, *Solid State Sci.* **2010**, *12*, 1881–1885.
[20] M. E. Amato, A. Licciardello, V. Torrisi, L. Ugo, I. Venditti, M. V. Russo, *Mater. Sci. Eng. C: Biom. Supramol. Syst.* **2009**, *29*, 1010–1017.
[21] C. Battocchio, I. Fratoddi, G. Iucci, M. V. Russo, A. Goldoni, Ph. Parent, G. Polzonetti, *Mater. Sci. Eng. C: Biom. Supramol. Syst.* **2007**, *27*, 1338–1342.
[22] I. Fratoddi, M. Delfini, F. Sciubba, M. B. Hursthouse, H. R. Ogilvie, M. V. Russo, *J. Organomet. Chem.* **2006**, *691*, 5920–5926.
[23] T. H. Schmitt, Z. Zheng, O. Jardetzky, *Biochemistry* **1995**, *34*, 13183–13189.
[24] R. J. Abraham, H. Pearson, K. M. Smith, *J. Am. Chem. Soc.* **1976**, *98*, 1604–1606.
[25] G. Iucci, G. Polzonetti, P. Altamura, G. Paolucci, A. Goldoni, M. V. Russo, *J. Vac. Sci. Technol. A* **2000**, *18*, 248–256.
[26] a) H. Takahashi, M. Kanehara, T. Teranishi, *J. Photopolym. Sci. Technol.* **2007**, *20*, 133–135; b) H. Imahori, H. Norieda, Y. Nishimura, I. Yamazaki, K. Higuchi, N. Kato, T. Motohiro, H. Yamada, K. Tamaki, M. Arimura, Y. Sakata, *J. Phys. Chem. B* **2000**, *104*, 1253–1260.
[27] M. Kanehara, H. Takahashi, T. Teranishi, *Angew. Chem. Int. Ed.* **2008**, *47*, 307–310.
[28] M. Zhou, S. Ouyang, Z. Liu, G. Lu, S. Gao, Z. Li, *Vibr. Spectrosc.* **2009**, *49*, 7–13.
[29] X. Liu, M. Atwater, J. Wang, Q. Huo, *Colloids Surf. B* **2007**, *58*, 3–7.
[30] H. Qian, R. Jin, *Nano Lett.* **2009**, *9*, 4083–4087.

[31] G. Polzonetti, C. Battocchio, A. Goldoni, R. Larciprete, V. Carravetta, R. Paolesse, M. V. Russo, *Chem. Phys.* **2004**, *297*, 307–314.
[32] J. J. Fischer, O. Jardetzky, *J. Am. Chem. Soc.* **1965**, *87*, 3237–3244.
[33] H. L. Anderson, *Tetrahedron Lett.* **1992**, *33*, 1101–1104.
[34] P. N. Taylor, A. P. Wylie, J. Huuskonen, H. L. Anderson, *Angew. Chem. Int. Ed.* **1998**, *37*, 986–989.
[35] T. Saito, H. Munakata, H. Imoto, A. Davison, K. Jonas, B. Albiez, *Inorg. Synth.* **1977**, *17*, 83–88.
[36] R. Vitaliano, I. Fratoddi, I. Venditti, G. Roviello, C. Battocchio, G. Polzonetti, M. V. Russo, *J. Phys. Chem. A* **2009**, *113*, 14730–14740.
[37] R. F. T. Stepto, *Polym. Int.* **2010**, *59*, 23–24.
[38] P. Swift, D. Shuttleworth, M. P. Seah, *Practical Surface Analysis by Auger and X-ray Photoelectron Spectroscopy* (Eds.: D. Briggs, M. P. Seah), Wiley, Chichester, **1983**, ch. 5 and appendix 3.
[39] D. A. Shirley, *Phys. Rev. B* **1972**, *5*, 4709–4714.
[40] G. E. Martin, A. S. Zekter, *Two-Dimensional NMR Methods for Establishing Molecular Connectivity*, VCH, New York, **1988**, p. 59.
[41] D. Neuhaus, M. P. Williamson, *The Nuclear Overhauser Effect in Structural and Conformational Analysis*, 2nd ed., VCH, Weinheim, **2000**.
[42] W. F. Reynolds, R. G. Enríquez, *J. Nat. Prod.* **2002**, *65*, 221–244.
[43] A. Ferri, G. Polzonetti, S. Licoccia, R. Paolesse, D. Favretto, P. Traldi, M. V. Russo, *J. Chem. Soc., Dalton Trans.* **1998**, 4063–4070.
[44] M. Brust, M. Walker, D. Bethell, D. J. Schiffrin, R. Whyman, *J. Chem. Soc., Chem. Commun.* **1994**, 801–802.
[45] F. Vitale, R. Vitaliano, C. Battocchio, I. Fratoddi, E. Piscopiello, L. Tapfer, M. V. Russo, *J. Organomet. Chem.* **2008**, *693*, 1043–1048.

Received: March 30, 2011
Published Online: September 14, 2011

